Development of a High Power 300 GHz Band Gyrotron for Practical Use in Collective Thomson Scattering Diagnostics in LHD

Teruo Saito[1], Jun Kasa[1], Yuusuke Yamaguchi[1], Yoshinori Tatematsu[1], Masaki Kotera[1], Shin Kubo[2], Takashi Shimozuma[2], Kenji Tanaka[2], and Masaki Nishiura[3]

[1] Research Center for Development of Far-Infrared Region, University of Fukui, Fukui 910-8507, Japan

[2] National Institute for Fusion Science, Toki 509-5292, Japan

[3] Graduate School of Frontier Sciences, The University of Tokyo, Kashiwanoha 277-8561, Japan

***Abstract*— A high power 300 GHz band pulse gyrotron has been designed and fabricated based the design concept for stable and single mode oscillation that has been experimentally verified with a prototype gyrotron. It will be practically use in the collective Thomson scattering (CTS) diagnostics in the Large Helical Device (LHD). The oscillation frequency is 303 GHz and the design calculation predicts stable oscillation of over 300 kW power at fundamental harmonic resonance.**

I. Introduction

Gyrotrons with frequencies around 100 GHz for electron heating are currently used in CTS diagnostics [1, 2]. However, the probe waves suffer from severe refraction and/or absorption in plasmas. Moreover, strong electron cyclotron emission (ECE) becomes a large noise source. Sub-THz waves are almost free from those problems. Therefore, a high power sub-THz gyrotron is required in CTS diagnostics in LHD. The probe wave power should be higher than 100 kW to realize a sufficient signal to noise ratio [3].

A second harmonic gyrotron was firstly tested. It demonstrated a high power, single mode oscillation and attained a power approaching 100 kW at 389 GHz [4, 5]. However, mode competition with a fundamental harmonic mode prevented to enhance the power [6]. Then, we have developed a fundamental harmonic prototype gyrotron and verified a design concept for stable single mode oscillation with a much higher power [7, 8]. By using the same design concept, a gyrotron for practical use in CTS diagnostics in LHD has been designed and fabricated. This paper reports the design calculation. Preliminary results of the oscillation test will be shown.

II. Design and Fabrication

The sub-THz gyrotron for CTS will be operated in a pulse mode. Therefore, a moderately over-moded cavity is used to satisfy simultaneously avoidance of mode competition and a low Ohmic loss on the cavity surface. The frequency of the practical gyrotron is 303 GHz. The oscillation mode is the $TE_{22,2}$ mode belonging to the same whispering gallery mode family as the $TE_{14,2}$ mode of the prototype gyrotron. The mode number has increased to meet a pulse width and a duty ratio up to 10 ms and 10%, respectively.

The left-hand side of Fig. 1 plots the dependencies of the oscillation power and the efficiency on the beam current I_B. The beam voltage V_k is 65 kV. An oscillation power higher than 300 kW is expected at I_B of 15 A with the pitch factor α of 1.2. Further higher power approaching 500 kW can be expected at

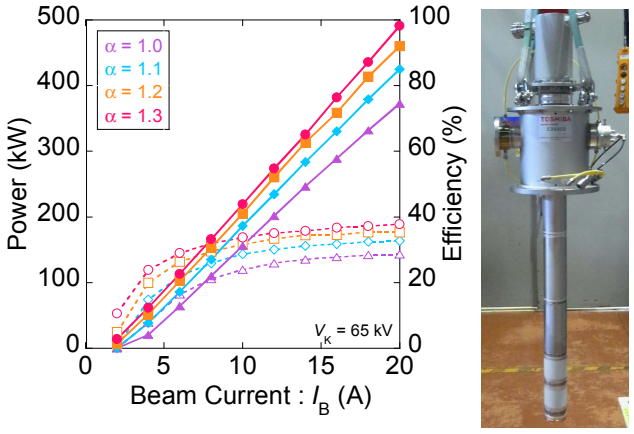

Fig. 1. (Left) Calculated oscillation power as functions of the beam current for several pitch factor. The beam voltage is 65 kV. (Right) Picture of the fabricated practical gyrotron. A Gaussian beam is radiated through the vacuum window at the left side.

I_B of 20 A with a practical value of α = 1.3. The oscillation efficiency is substantially higher than 30%. The average Ohmic loss density is lower than 1.4 kW/cm^2 for 300 kW and 10% duty ratio oscillation. The electron gun was newly designed and optimized for the $TE_{22,2}$ mode by using the same design principle as reported in Ref. [9]. An electron beam of high quality with the expected α values and sufficiently small velocity spreads can be generated up to I_B = 20 A [7].

This gyrotron is mounted on a liquid He-free 12 T superconducting magnet. The diameter of the room temperature bore is 100 mm. An internal mode converter is installed into a rather narrow room. The electron gun design is also compatible with the mode-convertor. The vacuum window is made from a single crystal sapphire disk of c-axis cut.

The gyrotron has been fabricated. A picture of the gyrotron is shown at the right-hand side of Fig. 1.

III. Initial Results of Oscillation Test

Oscillation test has just started. Figure 2 indicates the oscillation intensity as a function of the magnetic field strength B at the cavity. The oscillation intensity was measured with a pyroelectric detector placed in front of the vacuum window on the way of the beam radiated from the vacuum window. The beam radius was set at the maximum beam-wave coupling radius. This magnetic field dependence stands for V_k = 55 kV and at I_B = 9 A. The measurement was carried out with a pulse mode. The pulse width was 4 μs. The range of B very well

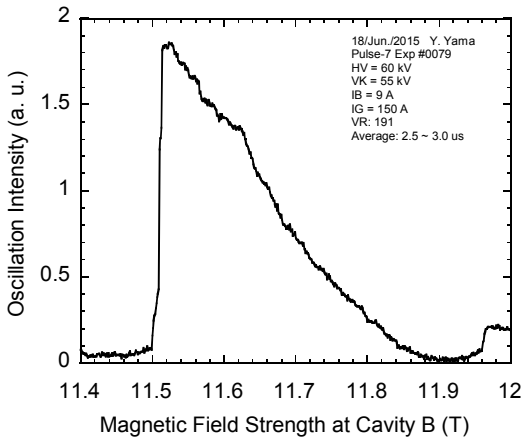

Fig. 2. Oscillation intensity measured with a pyroelectric detector placed in front of the vacuum window on the way of the radiation beam as a function of the magnetic field at the cavity. The beam voltage was set at 55 kV. The beam current was 9 A.

compares with that of the calculation, which indicates oscillation of the $TE_{22,2}$ mode.

The oscillation frequency was measured with a Fabry-Perot interferometer composed of two parallel meshes with a high reflection coefficient for the 300 GHz band. Figure 3 plots the transmission signal through two meshes as a function of the mesh distance for the case of $V_k = 60$ kV, $B = 11.55$ T. Narrow peaks appear very regularly with an identical interval. The oscillation frequency evaluated from the interval is 303 GHz. It is almost equal to the design frequency of the $TE_{22,2}$ mode. Then, the oscillation mode is definitely identified as the $TE_{22,2}$ mode. Moreover, the Fabry-Perot interferometer signal shows a pulse train with only one interval. This confirms single mode oscillation of the $TE_{22,2}$ mode.

The oscillation frequency was measured more accurately with a heterodyne receiver system. The measured frequency was 303.3 GHz for $V_k = 62$ kV, $B = 11.59$ T. It is almost equal to the design frequency within an accuracy of the order of 10 MHz. The frequency variation due to variation of the operation conditions was less than ±100 MHz.

The radiation pattern was measured with an infrared camera.

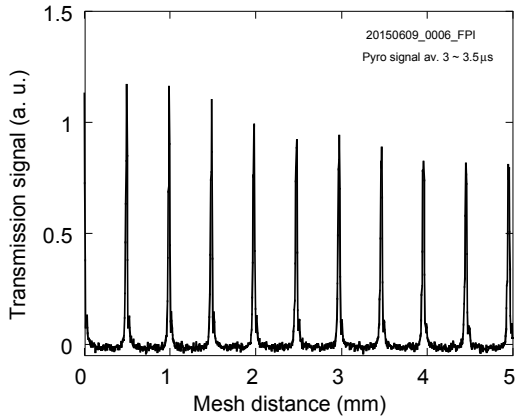

Fig. 3. Transmission signal of the Fabry-Perot interferometer as a function of the distance between two parallel meshes.

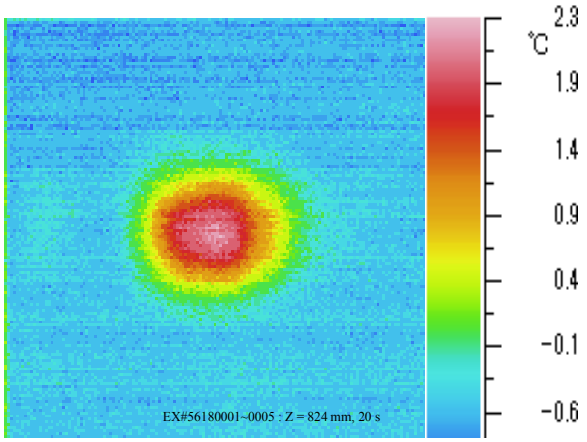

Fig. 4. Radiation pattern measured with an infrared camera. The distribution of the temperature increase on a poly vinyl chloride plate is shown. The distribution stands for the radiation pattern. Measurement was carried out for a short pulse mode. The infrared camera image covers an area 100 mm x 100 mm.

Figure 4 represents a profile of temperature increase of a 1 mm-thick poly vinyl chloride (PVC) plate put in front of the vacuum window vertically to the radiation beam. The distance between the vacuum window and the PVC plate was 60 cm. A well collimated Gaussian like radiation pattern was observed. This pattern is very similar to the calculated one. The mode converter installed in a very narrow space works well.

A preliminary measurement of the output power was carried out with a water load installed in a circular waveguide connected from the vacuum window with a taper and a miter bend. More than 200 kW has already been obtained for $V_k = 60$ kV and at $I_B = 15$ A. Optimization effort to confirm 300 kW will be made.

IV. Summary

A 300 GHz band pulse gyrotron was designed based on the same concept of the prototype gyrotron and fabricated for actual use as a power source of CTS diagnostics in LHD. The initial results of the oscillation test has confirmed single mode oscillation of the $TE_{22,2}$ mode as the design mode. The measured frequency is almost equal to the design value, which corresponds to a minimum of ECE for the standard operation of LHD. The radiated beam has a well collimated Gaussian like pattern. More than 200 kW has been obtained. Over 300 kW oscillation will be obtained after optimization of the operation conditions.

References

[1] Bindslev *et al.*, *Phys. Rev. Lett.* **97**, 205005, 2006.
[2] M. Nishiura *et al.*, *Nucl. Fusion* **54**, 023006, 2014.
[3] T. Saito et al., *Journal of Phys.: Conference Series* **227,** 012013, 2010.
[4] T. Notake, et al., *Phys. Rev. Lett.* **103**, 225002, 2009.
[5] T. Saito *et al.*, *Phys. Plasmas* **19**, 063106, 2012.
[6] T. Saito *et al.*, *Phys. Rev. Lett.* **109**, 155001, 2012.
[7] T. Saito et al., *IWMMW-THz 2014*, R3/D-25.17, Tucson, USA, Sept. 14-19, 2014.
[8] Y. Yamaguchi et al., *Nucl. Fusion,* **55**, 2015, 013002.
[9] Y. Yamaguchi *et al.*, *Phys. Plasmas* **19**, 113113, 2012.